Ion-Neutral Clustering Alters Gas-Phase
Hydrogen-Deuterium Exchange Rates

Authors: Haley M. Schramm, ¹ Tomoya Tamadate, ² Christopher J. Hogan, ² Brian H. Clowers ¹

¹Department of Chemistry, Washington State University, Pullman, WA 99163, USA

²Department of Mechanical Engineering, University of Minnesota, Minneapolis, MN 55455, USA

The rates and mechanisms of chemical reactions that occur at a phase boundary often differ

Abstract

dynamics.

considerably from chemical behavior in bulk solution, but remain difficult to quantify. Ion-neutral interactions are one such class of chemical reactions whose behavior during the nascent stages of solvation differs from bulk solution while occupying critical roles in aerosol formation, atmospheric chemistry, and gas-phase ion separations. Through a gas-phase ion separation technique utilizing a counter-current flow of deuterated vapor, we quantify the degree of hydrogen-deuterium exchange (HDX) and ion-neutral clustering on a series of model chemical systems (i.e. amino acids). By simultaneously quantifying the degree of vapor association and HDX, the effects of cluster formation on reaction kinetics are realized. These results imply that cluster formation

Keywords: Molecular Solvation; Ion Chemistry; Hydrogen-Deuterium Exchange; Gas-Phase Ions; Ion-Molecular Reactions; Ion Mobility; Mass Spectrometry

cannot be ignored when modeling complex nucleation processes and biopolymer structural

Introduction

The quantitative accounting of ion-neutral and ion-ion reactions have direct impacts across disciplines including atmospheric chemistry, 1,2 structural biology, 3 catalysis, 4 plasma physics, 5 and astrochemistry. 6-8 Not only can ions drive chemical reactions in natural systems (e.g. ion-induced nucleation), 9,10 but also many of the foundational principles in chemical reaction theories are tested via examination of gas phase ion-neutral reactions. 3,9,11–13 It is also interesting to note that clustering properties (e.g. enthalpy and entropy) during particle growth are often distinctly different than behavior in bulk solution, further emphasizing the need to quantitatively evaluate ion-neutral interactions during the nascent stages of cluster growth. For example, compared to bulk solutions, reaction rates are often greatly enhanced in clusters and microdroplets, which has direct bearing on models integrating aerosol size and chemical kinetics. 14,15 The imperative to comprehensively probe solvation and clustering behavior is further bolstered by recent reports of the capacity for small droplets to induct drastic changes in localized pressure and alter chemical reactivity. 16

Historically, clustering of ions and neutrals has been probed by a range of spectroscopic techniques. 17-23 Using these approaches, researchers have quantified a range of fundamental properties and even demonstrated the capacity to differentiate between stochastic and preferential clustering behavior using thermodynamic arguments. 24,25 The latter remains particularly relevant when developing models to predict the behavior of macromolecule solvation and nucleation. As the focus on particles and aerosols narrows, questions surrounding the nucleating events between ions and neutrals arise. The importance of these events with respect to climate change and the natural environment are readily apparent, however, there are yet additional disciplines beyond atmospheric science where the role of ion solvation remains critical.

Biopolymers (e.g. carbohydrates, proteins, and their composites) remain the focus of efforts in structural biology that probe conformational changes of macromolecules with respect to the external environment. Solution and solid phase techniques (e.g. NMR and x-ray crystallography) remain essential in these pursuits, but high mass spectrometry approaches continue to provide unique insights into the dynamism displayed by proteins and their conjugates. In fact, a recent coupling of mass spectrometry and transmission electron microscopy (TEM) illustrates the potential for gas-phase measurements to inform solution phase behavior.²⁷ Such measurements are also complemented by relatively mature approaches to infer gas-phase protein structure through hydrogen-deuterium exchange (HDX) techniques.^{28–30} These approaches can provide direct experimental evidence for which amino acid residues are solvent accessible and rationally constrain folding models.^{31,32} Despite these highly granular experiments, gas-phase measurements of biopolymers rarely explore the role of nascent solvation on conformation (i.e. interactions with just a few solvent molecules). An experimental technique that allows bare ions to locally solvate to form a cluster presents a considerable opportunity to detail the sites of solvation and the conformational changes induced during clustering.

HDX experiments traditionally fall into two different categories: bulk solution HDX experiments and low-pressure gas-phase HDX. In bulk solution, higher order biopolymer structure is assessed by solvent exposure of amino acid residues. Similar structural inferences have been obtained via gas-phase HDX. Gas phase workflows may reduce reaction times but also increase tunability in the deuterium source used. Solution exposure is limited to D₂O whereas gas-phase experiments have employed deuterated ammonia, methanol, and acetic acid to name a few.³³ The mechanism by which the deuterated modifier exchanges with the analyte is dependent upon the difference in proton affinity between the two via a long-lived ion-neutral complex of either one or two hydrogen bonds.³³ For this reason, HDX experiments can be thought of as a subset of ion-neutral clustering

experiments that are particularly interesting when using a mass spectrometer so isotopologue intensities can be monitored.

The first gas-phase HDX experiments were done in trapping mass spectrometers. These experiments require very low pressures (~10-7 torr) that restrict deuterium incorporation and pose challenges for quantification. Ion mobility is a complementary gas-phase technique commonly used for similar structural studies as HDX-MS but can be done at higher pressures. Valentine and Clemmer first demonstrated the utility of gas-phase HDX within an ion mobility cell using a comparatively high pressure (~2 torr) drift tube IM-MS.34,35 Their work showed the richness of the data obtained from the simultaneous ion-neutral reactions and complementary instrumental detection. Still, restrictions imposed by the reduced pressures of the deuterated water, quantitative results and low deuterium incorporation remained an obstacle.

While both of these innovative approaches highlight the importance of the long-lived ion-neutral complex to facilitate HDX, neither observe or quantify the effects of clustering and obtain an exchange comparable to bulk experiment. To quantitatively capture the physical and thermodynamic parameters that influence the degree of ion-neutral clustering and HDX, new analytical methods are necessary that mitigate the challenges associated with traditional approaches to probe gas ion-neutral interactions under vacuum conditions. In addition to higher collision frequency, the previously discussed HDX-IMS data sets can be more informative using a site-specific clustering species. Prior work by Oberreit et al.,20 and affirmed through subsequent measurements in our own laboratory, suggest that H2O typically participates in non-specific clustering with subnanometer scale ions, which informed the selection of an alternative vapor modifier in the present work.

To demonstrate the influence of cluster formation on ion-neutral reaction rates, using an innovative combination of atmospheric pressure ion mobility with counter-current flow of

deuterated vapor with site-specific clustering behavior and mass spectrometry, here we examine hydrogen-deuterium exchange (HDX) reactions between amino acid ions and deuterated methanol as a model ion-neutral system. Critically, the extent of HDX and the degree of ion-neutral clustering are simultaneously monitored using the experimental apparatus with ion mobility measurements quantifying changes in ion-neutral clustering and mass spectrometry monitoring the levels of HDX. These foundational efforts highlight the utility of increased collision frequencies to probe HDX rates for protons that are rarely observed in reduced pressure experiments and correlate the degree of ion-neutral clustering with different exchange rates. We describe the experimental methods employed, and results towards understanding clustering influences on HDX reactions in the subsequent sections.

Experimental Procedures

The experiments performed build upon the approach of Kwantwi-Barima *et al.*, who demonstrated a gas-phase ion mobility method for characterizing energetics of ion-vapor clusters by directly equating shifts in ion arrival time distributions with the degree of clustering between a target ion population and the neutral condensable vapor.^{25,36,37} Importantly, the results by Kwantwi-Barima *et al.* provide a direct link between vapor-induced shifts observed in the mobility domain and the thermodynamics of selective interactions between ions and neutrals which directly contribute towards the broader process of nucleation.²⁴ From these cited works, several characteristics of the clusters at ambient temperature and pressure can be carried to the present study: clusters are transient between the bare ion and a singular vapor molecule and, as the concentration of modifier is increased, persist longer and longer. The assumption of a single vapor molecule transiently binding is supported by the modest shifts in mobility (<10%) brought about by vapor introduction; prior work reveals substantially larger shifts in mobility (reduced by a factor of 2) for

sub-nanometer scale to nanometer scale ions if multiple vapor molecules bind.38 Furthermore, the noncovalent interactions between the binding vapor molecule and ion are disrupted upon transfer from the atmospheric pressure drift cell through the vacuum interface of a mass spectrometer,39 wherein inlet electric fields lead to acceleration of ions to elevated speeds.40

Sample Preparation. Amino acids were purchased from Sigma-Aldrich Chemical Co. (Milwaukee, WI). Stock solutions for select amino acids were prepared by dissolving in DI H2O and stored at 5 °C. Structures for the amino acids included are shown in Figure 1. Working electrospray solutions were prepared fresh daily from stock solutions using 95/5 acetonitrile/DI H2O with 0.1% formic acid to 100 μ M for methionine, 75 μ M for tryptophan, and 200 μ M for glycine, serine, and cysteine. Cocaine was included at 1 μ M as a system suitability check for ion mobility calculations in all electrospray solutions to ensure any variability in the arrival time distribution of the amino acids was due to chemical variability (e.g. clustering) rather than instrumental drift or environmental factors.

Work by Mortensen and Williams showed that a droplet's lifetime is, at most, tens of microseconds.41 Since the ions spend tens of milliseconds in the drift tube, the percentage of time spent as an ESI solvent droplet interacting with the modifier vapor is negligible. The mobility for cocaine utilized as a system check is also further evidence ions are fully desolvated after electrospray. Then, upon addition of the reactive modifier, transient clusters form between the bare ion and, in this case, deuterated methanol. Previous work has shown the mechanism of exchange between the [M+H]+ amino acid ions and deuterated methanol through a long-lived ion-neutral complex.33,36,42,43 We consider the system of exchange and clustering between one ion and one reactive modifier; as noted above, mobility shifts brought about by vapor clustering are modest, suggest at most one vapor molecule remains to the ion during measurement, and hence any incoming modifier encounters either a bare ion, or an ion with a single vapor modifier bound at most. Though subtle, this is distinctly different from the work of

several others examining reactions in microdroplets. An "exchange competent" complex for this system, as previously documented, is one with two hydrogen bonds between the amino acid and the methanol.33,44,45 Schematics of the hydrogen bonded complex can be found in Figure S2 as well.

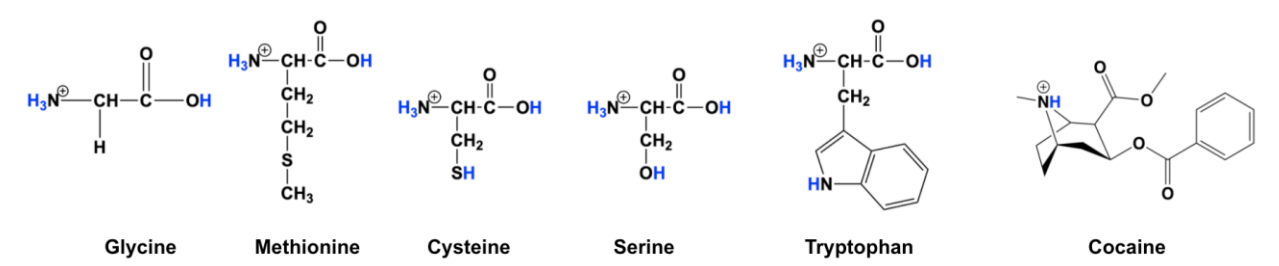


Figure 1: Analyte structures for comparison. All amino acids have at least 4 exchangeable hydrogens (three from protonated amino group and one from the COOH) while cocaine only has one from the protonated amino- group. Theoretically exchangeable hydrogens are labeled in blue.

experiments were performed using an atmospheric pressure, dual gate PCB drift tube ion mobility spectrometer (IMS) coupled to a LTQ XL (Thermo Fisher Scientific, Thousand Oaks, CA). 46,47 A schematic of the instrumentation is shown in **Figure 2**. The drift gas, nitrogen, is introduced into the drift tube just before the entrance of the MS. Ions are spatially separated by their reduced mobility coefficient, K0, before mass analysis. The IMS unit is securely mounted to the MS inlet and, while not explicitly gas-tight, the positive pressure from the countercurrent flow of gas prevents exposing the system to the external laboratory environment (i.e. no appreciable water content is introduced into the system).

Working solutions were electrosprayed at 3 μ L/min into the IMS using a 75 μ m ID glass capillary using an applied potential of 2.2 kV above the entrance potential of the IMS. The drift tube was operated at atmospheric pressure and room temperature (~700 torr and 24 °C in Pullman, WA). Mass-selected mobility spectra were extracted by encoding the data in the frequency domain and using Fourier transform as described previously as shown in Figure 3.48 The synchronized gates were pulsed using a frequency sweep from 5 Hz to 8005 Hz over 430 seconds. The countercurrent

drift gas was N2 at 2.75 L/min modified with 99% pure methanol-OD (CH3OD, (Cambridge Isotope Laboratories, Inc. (Andover, MA)) through the primary gas inlet at variable flow rate between 5 and 300 µL/hr using a syringe pump. Under these conditions, the MeOD is approximately 0.1% of the drift gas ensuring that the modifier is not abundant enough to induce any noticeable effect (e.g. ion mobility within MeOH or polarizability effects) other than a shift in the resident time of the ions in the drift tube through transient ion-neutral clusters. The shifts in mobility that arise from a shift in drift time were assessed by calculating Ki/Ko ratio where Ki is the mobility of the amino acid with some concentration of modifier introduced into the drift gas and Ko is the mobility of the amino acid with no modifier as presented previously.49 A ratio of 1 is indicative of situations where the modifier does not interact with the target analyte.

To extract kinetic data from the isotope window, we utilized two different approaches. First, semilog plots were prepared to linearize the data and calculate rate constants in accordance with pseudo-first order kinetics.34,50,51 The linear form of the pseudo-first order kinetics integrated rate law is shown in Equation (1) where [Hex] is the number of remaining hydrogens with some concentration of modifier, [CH3OD] is the pressure of the modifier in torr, k is the rate coefficient, t is the total time the amino acid is exposed to the modifier and [Hex]0 is the number of remaining hydrogens with no modifier present.

$$ln[H_{ex}] = -[CH_3OD]kt + ln[H_{ex}]_0$$
 (1)

Average m/z values for each amino acid replicate with variable CH3OD flow rates were calculated by a weighted average of the intensities and m/z values in the isotopic window. The number of remaining exchangeable hydrogens was calculated by subtracting the average m/z from the m/z if all theoretically exchangeable hydrogens were deuterons. Since there is only one exchangeable deuterium on the modifier, a successful exchange will produce CH3OH. The countercurrent flow

ensures the non-deuterated methanol created is carried in the opposite direction from deuterated species, virtually eliminating the opportunity for back-exchange. Each modifier flow rate was analyzed at 3 different electric field strengths ranging from 533 to 583 V/cm to ensure reproducibility. Details of the second kinetics data analysis approach and other experimental parameters are provided in the supporting information.

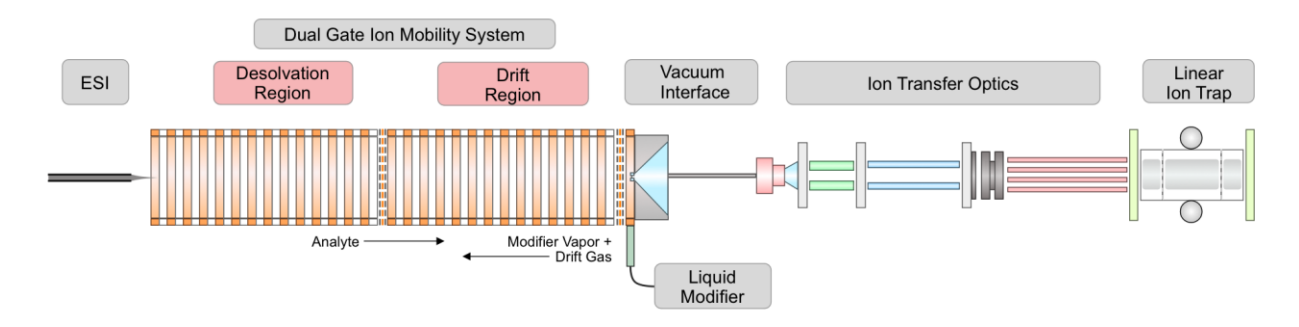


Figure 2: Simplified instrumental set up of the atmospheric pressure, dual gate ion mobility spectrometer coupled to a LTQ mass spectrometer. The sample solution is introduced via electrospray into the drift tube. Ion packets are pulsed into the drift region through the first gate and are separated by mobility. Mobility spectra are obtained by encoding the data in the frequency domain. The frequency encoded mobility spectra may be used to recover drift time spectra for m/z selected ions using fast Fourier transform. Changes in isotope distribution are monitored by the LTQ as a function of modifier flow rate. The modifier is introduced through the primary drift gas inlet through a GC injection liner at variable flow rates using a syringe pump.

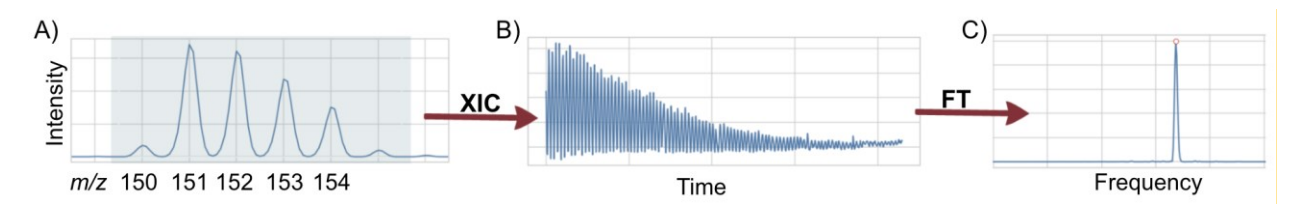


Figure 3: Sample data processing scheme for methionine. A) A sample mass spectrum with CH₃OD with the isotopic window highlighted. The m/z 150 is the monoisotopic mass of the singly charged amino acid which has 4 exchangeable hydrogens. The peak at m/z 155 is from 13C naturally occurring. B) The mass-selected ion chromatogram from the highlighted isotopic window. C) The recovered mobility peak. The frequency is converted to a drift time by the sweep rate of the synchronized gates.

Results and Discussion

Correlating Degrees of Ion-Neutral Clustering and HDX.

A brief overview of the data produced by the integrated HDX and ion-neutral clustering experiment is warranted. Figure 4 condenses the behavior of the analyte isotopic envelope as a function of CH₃OD concentration along with the degree of ion-neutral clustering observed and the total observed exchange rate(s). Specifically, Figure 4A captures the normalized intensity of the respective isotopes of methionine as a function of vapor modifier concentration. Figure 4B shares a common x-axis with Figure 4A but transforms the individual intensities of the isotopologues described by a semilog pseudo-first order kinetics equation to yield the observed HDX rates across experimental conditions. Additionally, the rightmost axis of Figure 4B corresponds to the degree of ion-neutral clustering observed. The piecewise linear fits shown in Figure 4B were data driven to optimize the degree of linearity between the two distinct exchange rates (e.g. fast vs. slow (shallower slope)) using the *pwlf* python package. 52 The breakpoint is the location along the x-axis in the semilog plots calculated to be the end of the first linear segment (the fast rate) and the beginning of the second (the slow rate) signified by the vertical dashed line. A key observation in this effort is that two distinct HDX rates were observed for all of the amino acids probed. Additionally, the breakpoints between rates is also highly correlated with the degree of ion neutral clustering with a sharper decrease in y-axis at lower flow rates and a more gradual slope at higher flow rate. This correlation prompts a range of questions relating the rate-limiting HDX factors to the degree of clustering and also the notion that multiple disparate exchange populations simultaneously exist within an ion-neutral cluster and within the drift cell. Quantitative results are tabulated in Table S1. Alternative analysis through fitting to a population balance model, leading to the same conclusion that HDX rates shift with increase vapor modifier pressure, is also discussed in the supporting information (Figure S7).

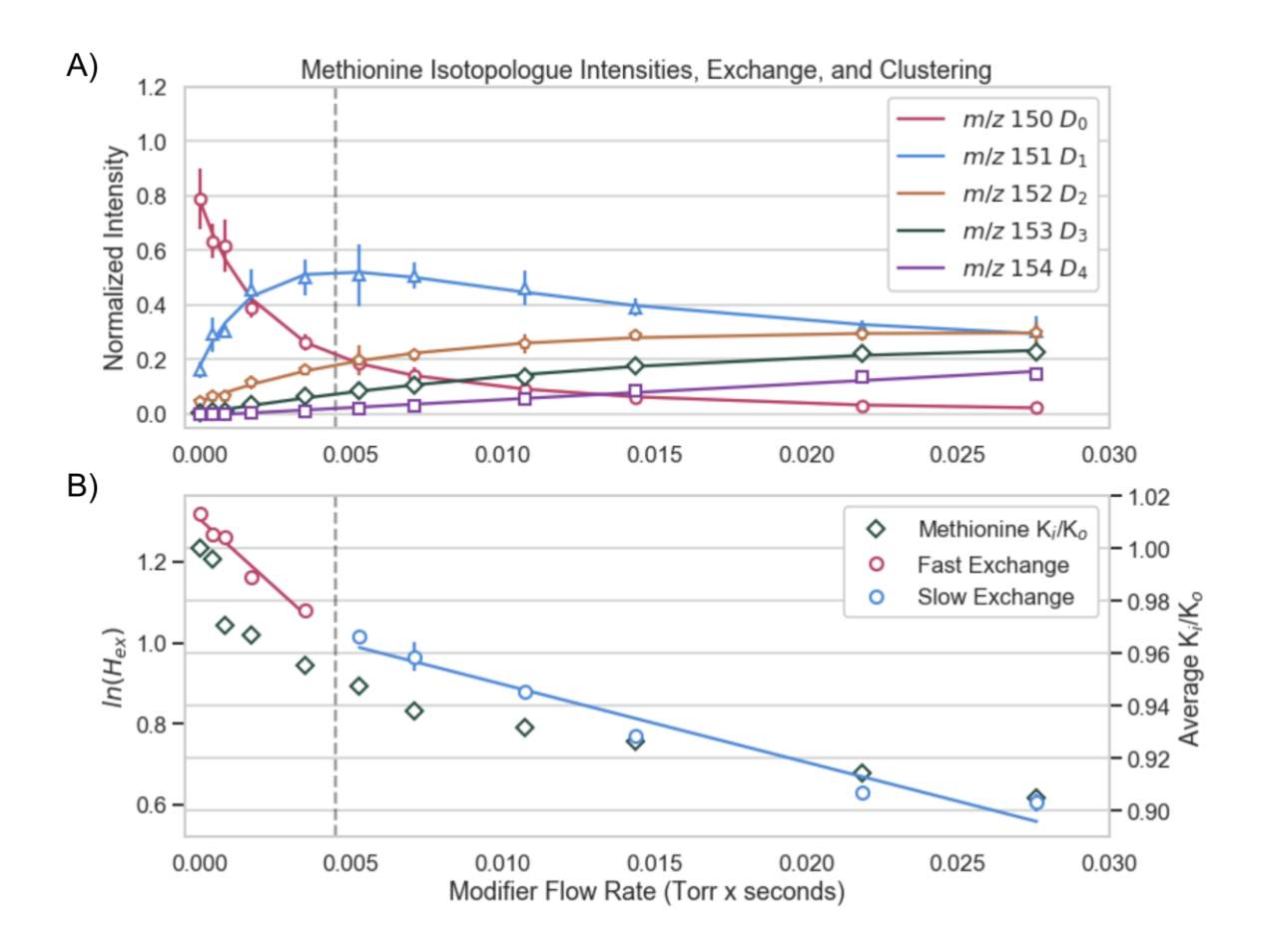


Figure 3: A) Methionine isotopologue intensity with a double exponential fit and B) semilog plot calculated from the average number of remaining hydrogens as functions of modifier flow rates (pink and blue circles with linear fit). Clear site-specific ion-neutral clustering can be observed in the mobility shifts (dark green diamonds).

Impact of Chemical Functional Groups on HDX

The mechanisms by which deuterating agents exchange with available hydrogens has been studied previously. 33,53–55 In accordance with well-established literature in the fields of reduced and high-pressure mass spectrometry, when the difference in proton affinity between the deuterium source and the amino acid is less than 20 kcal/mol, a strong hydrogen bond forms allowing for exchange. 33,54,55 However, when the difference in proton affinity is greater than 20 kcal/mol, the exchange is impeded by an endothermic proton transfer, and a second hydrogen bond must be formed to lower the barrier and allow for exchange to occur. Because all of the selected amino acids exhibit proton affinity differences greater than 20 kcal/mol (see Table 1),

this double hydrogen bond mechanism is the likely mechanism for exchange in this work. Schematics of this ion-neutral complex are provided in **Figure S2**. While this mechanism is likely to dominate, the repeated observation of two distinct rates for the amino acids probed suggest that as ions exist more and more in clusters, the rate of exchange is altered. Before pursuing this concept in more detail, exploring the role of different chemical functionality on the degree of ion-vapor clustering and HDX rates are needed since different functional groups have been postulated as the origin of pseudo-first order nonlinearity.

Table 1: Summary of the analytes used to investigate HDX behavior with methanol-OD.

Analyte	<i>m/z</i> [M+H] ⁺	# Theoretical H _{ex}	# Observed H _{ex}	ΔProton Affinity (kcal/mol) ^A
Tryptophan	204	5	4	46.67
Methionine	150	4	4	43.04
Cocaine	304	1	0	42.18
Serine	106	5	5	38.29
Cysteine	122	5	4	35.56
Glycine	76	4	4	31.60

^AThe proton affinities for the amino acids and methanol were obtained from the NIST database. The proton affinity for cocaine has been reported previously. ⁵⁶ The differences between the proton affinity of methanol and the analytes were calculated.

The isotopologue data for methionine (Figure 4A) suggests site-specific exchange could possibly be the cause of more than one rate coefficient observed since the D0→D1 exchange constitutes the majority of the fast exchange prior to the breakpoint. However, data from the methionine methyl ester (Met ME) which also exhibits nonlinear kinetics though only one type of exchangeable hydrogen is available. This strongly suggests that the order in which hydrogens exchange is not fixed (Figure S3), and site-specificity is not the sole cause of nonlinearity in the pseudo-first order semilog plots. A similar conclusion was obtained previously supporting that the

rate constants reported from this type of experimental approach are average exchange rates resulting from "exchange competent" ion-neutral complexes that form as ions traverse the drift tube.⁵⁷ The exchange rates calculated for the methyl ester are slower than methionine indicating that while the carboxylic acid does indeed react faster than the amine group hydrogens, it is not the sole reason for the two rate observation. This implies, at least for our data sets, the fast rate cannot be implicitly attached to the carboxylic acid exchange and the slow rate to the amino group exchanges. When viewed from a slightly different perspective, it is important to recognize that the observed rates must arise from a mixture of ion populations with varying degrees of HDX reactivity, highlighting that the species detected and spectra used to calculate the isotopic profile is an average of variably-exchanged ions.

Extending this concept further, cysteine and serine can be considered. While the labile hydrogens in cysteine rapidly exchange, the system approaches a steady-state during the course of the experiment (Figure 4A). Four of the five hydrogens exchange for cysteine whereas all five labile hydrogens exchange for serine. This is rationalized by the inability of cysteine's sulfhydryl side to stabilize a hydrogen bond long enough to enable exchange. Still, greater exchange is observed in this work than previously reported demonstrating an advantage of higher pressure analysis.45 The average rates for cysteine are faster than the average rates calculated for methionine suggesting the side chain effects exchange kinetics. Further experiments are necessary to confirm these speculations.

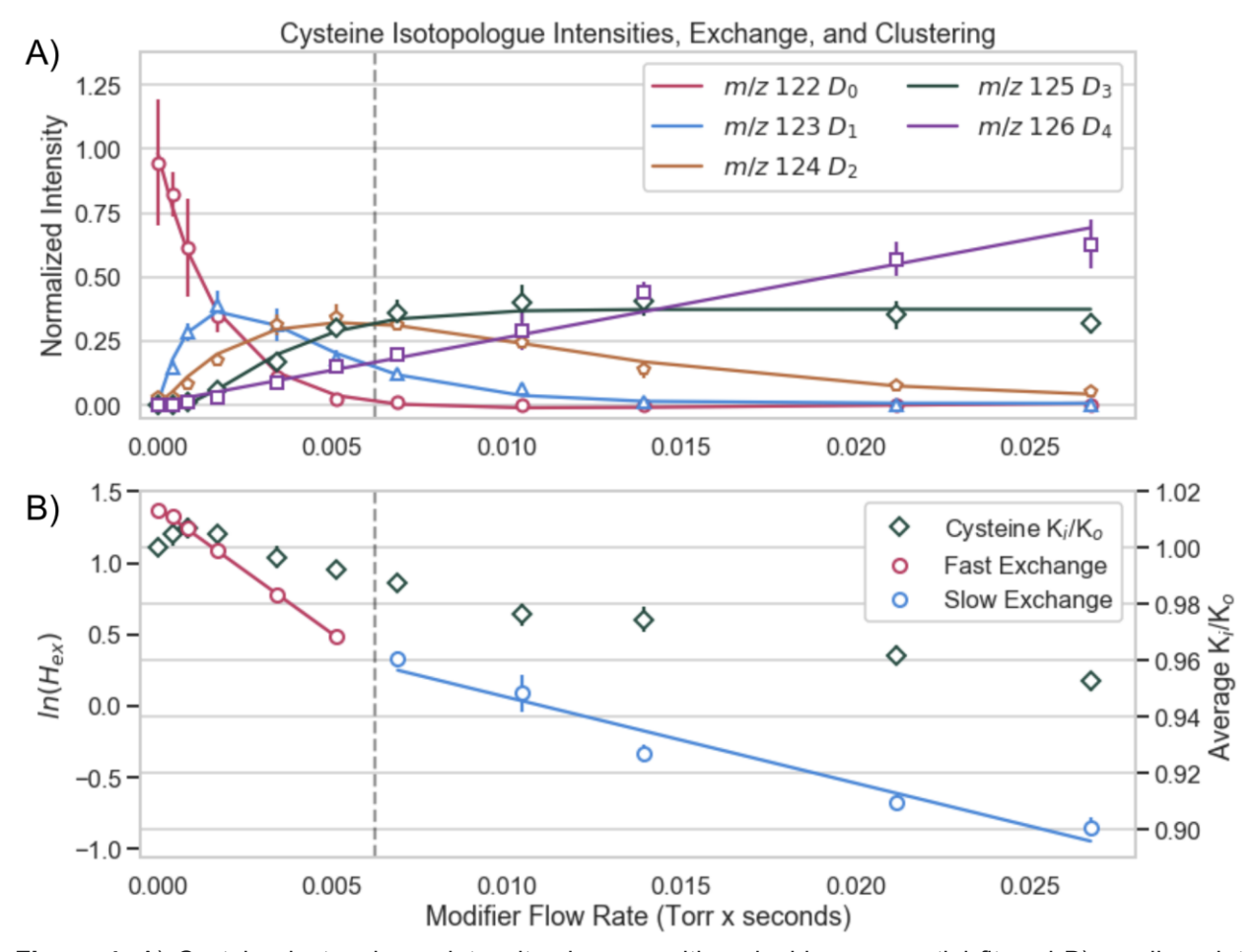


Figure 4: A) Cysteine isotopologue intensity changes with a double exponential fit and B) semilog plot calculated from the average number of remaining hydrogens (pink and blue circles with linear fit). The ion-neutral clustering can be observed in the mobility shifts (dark green diamonds).

To this point in the discussion, our data illustrate that more than one exchange rate is present but the degree of ion-neutral clustering has yet to be explored. A key advantage of the present HDX workflow is its capacity to quantify the degree to which an ion population clusters with the exchange partner. Following observations that suggest that vapor uptake by peptides is site-specific and unique to the analyte/modifier pair, it can be rationalized that amino acids would exhibit similar behavior.^{24,37} The degree of ion-vapor clustering is explicitly embedded in the observed shifts in mobility. Returning to the comparison of the methionine (**Figure 4B**) and methionine methyl ester (**Figure S3B**) clustering plots, it is clear that the carboxylic acid group present on methionine is integral to the formation of clusters. Evaluation of the observed shifts in

mobility (i.e. green diamonds) for methionine methyl ester illustrates that a minimal amount of clustering occurs during the experiment, whereas, methionine displays shifts in mobility that approach 10% across the vapor modifier conditions used. Additionally, the difference between the exchange rate slopes for methionine are considerably more pronounced. This comparative analysis provides evidence that the rate of HDX exchange could be correlated with the degree of vapor-ion clustering.

Table 2 compares the absolute mobility shifts calculated for each amino acid and the degree of HDX reactivity. There was no trend observed between proton affinity and exchange or the absolute mobility shifts. The data show that the computationally determined breakpoint in the observed HDX rates is inversely related to the extent of ion-neutral clustering. For example, the breakpoint for methionine was observed to occur at the lowest CH₃OD flow rate of the amino acids probed but exhibits the largest mobility shift, upwards of 10%. On the other hand tryptophan's breakpoint was found at the highest modifier flow rate and this ion population exhibited negligible ion-neutral clustering behavior (< 3% shift in gas-phase ion mobility). Interestingly, cysteine, serine, and glycine displayed similar degrees of mobility shifts but different points were observed for the breakpoint location.

Analyte	Maximum Relative % Shift	Breakpoint Location (Torr x s)	
Methionine	9.6 ± 0.5	0.0045	
Glycine	5 ± 1	0.0048	
Cysteine	4.7 ± 0.3	0.0062	
Serine	4.8 ± 0.3	0.0107	
Tryptophan	2.8 ± 0.5	0.0124	
Met ME	1.9 ± 0.8	0.0081	

Table 2: Comparison between the maximum percent mobility shifts and calculated breakpoint locations for each amino acid. The maximum shift is the percent change in the mobility at the highest concentration of modifier in the drift cell and the error is the standard deviation.

While select reports for both FT-ICR and reduced pressure drift cell experiments note the presence of multiple rates, this observation is far from universal. For all of the amino acids probed in this effort, multiple rates were observed with increased levels of D incorporation compared to lower pressure experiments. To place the present work in context, prior work by Gard et al. probed a similar set of amino acids using CH₃OD using an FT-ICR. They similarly identify exchange occurs faster on the carboxylic acid but that the exchange on the different functional groups maintains some level of independence.⁴⁵ However, due to low pressure constraints, only two exchanges for cysteine and serine are observed.⁵³

Though the degree of clustering and HDX is quantitative, the exact orientation of the ion with the reactive vapor remains unknowable with just the present set of experiments. Nevertheless, the quantitative aspects of this work establish that, at a minimum, 4 different scenarios exist with respect to ion-neutral clustering and HDX. These condensed scenarios place bounds on the possible interactions that occur during a gas-phase HDX experiment. The simplest scenario involves conditions where no HDX is observed and no clustering is exhibited. Conversely, the scenario also exists where a purely gas-phase mechanism where HDX is observed but no

clustering (i.e. no shift in mobility). The remaining two possible conditions include scenarios where clustering does occur coupled with and without HDX. **Figures S9-S10** graphically capture this concept for all of the amino acids probed. While relative in nature, these comparisons illustrate that conditions where clustering occurs and HDX does not occur are improbable. In this regard, this comparative exercise combined with our experimental data suggest that clustering, even if brief, does indeed play a considerable role in HDX.

Conclusions

HDX within the amino acid/CH₃OD complex requires two hydrogen bonds to form due to the difference in the proton affinities³³ and occurs via a long-lived intermediate.⁴³ Because of this, it can be theorized why there is a clear connection between the degree of exchange and the extent of ion-clustering that includes an exchange partner. However, since a transient cluster can be formed that is not "exchange competent," other possible cluster orientations that contribute to the shifts in mobility exist (e.g. only one hydrogen bond). This illustrates the complementary nature of these reactions. Transient clusters not capable of exchange may alter the observed mobility while exchange competent reaction complexes may not survive long enough to alter the mobility, highlighting the interesting nature of correlating mobility shifts and HDX kinetic nonlinearity.

When viewed within the context of the large body of work focusing on gas-phase HDX, the integrated workflow presented here can aid in quantifying the degree to which an ion-neutral cluster exists and for how long. Though a subtle point, shifts in gas-phase mobility are due to transient vapor interactions that occur under equilibrium conditions, but the strength of these intermediates is insufficient to survive the pressure differential to vacuum required for mass spectrometry. Prior experiments conducted at low pressure cannot realize the same degree of ion-neutral clustering, and by extension HDX, that is observed in the present atmospheric

pressure drift tube experiment.

The observation of multiple kinetic rates within the semilog plot using pseudo-first order kinetics is usually attributed to site-specific exchange. For this reason, methionine and methionine methyl ester were compared to see the effects of higher pressures of this interpretation. Using conventional HDX interpretations, we would expect the methyl ester semilog plot to host a singular linear relationship with a rate constant the same as the "slow" rate observed in methionine. However, the multiple rate semilog plot holds for the methyl ester, meaning a difference in site specific HDX rates cannot be the sole reason for nonlinearity. Comparing the respective fast and slow rates of methionine and methionine methyl ester, we see that both rates measured for methionine methyl ester are slower than methionine. This suggests that, while the carboxylic acid exchange is faster than the amino group exchange as predicted by several previous publications, measured rates with this technique are not implicitly the rate of exchange for the carboxylic acid and the amino group, but rather a mixture of ions with a variety degrees of exchange.

Additionally, the rates of exchange obtained in this study are lower than previously reported (see Table S1). 44,53 The formation of ion-neutral clusters may slow down observed rates. 43 These cited studies attempt to measure site-specific rate constants whereas the rate constants reported here are averages of all the exchanges that occur as D₀ reacts to form D₁ and so on which we have shown cannot explicitly be attributed by one reactive site. However, the order of magnitude is similar between the rate constants from literature and reported here (10⁻¹¹ cm³ molecule⁻¹ s⁻¹) with much lower percent error demonstrating the utility of the liquid introduction of deuterated vapor. The greatest error was calculated for the slow rate of tryptophan which is due to the lack of points used in the linear regression since the breakpoint is at relatively high modifier pressures.

Though the exchange data obtained are not site-specific rate constants, the comparison between methionine and its methyl ester derivative illustrates analyte/modifier functional specificity of both

HDX and ion-neutral clustering that will be useful in future studies. Further investigation into the cause of nonlinearity will be conducted in subsequent work to examine the effects of temperature, derivatized amino acid structure, and the kinetic isotope effect on reactivity. 35,58 Supplemental molecular dynamics simulations may also support experimental findings and perhaps provide more insight into these complex gas-phase ion-neutral reactions.

The low pressure essential to previous gas-phase HDX techniques restricts the range of the x-axis (Torr x seconds) for the kinetic plots excluding experiments at higher modifier pressures. The data set obtained by this workflow in the higher pressure regime shows the behavior of exchange kinetics is a function of the concentration of the modifier. An increased dynamic range for HDX experiments is thus advantageous. By eliminating the possibility of back exchange by using CH₃OD and proceeding the reaction at much higher collision frequency, the presented experimental workflow offers a promising opportunity to further exploit previously excluded phenomena in ion mobility: gas-phase reactions and ion-neutral clustering. Reasonable HDX rate coefficients with less intrinsic experimental error were obtained for five different amino acids of biological relevance and linked to ion-neutral clustering behavior.

In addition to the direct applications of this technique in atmospheric chemistry, this work also demonstrates the utility of this method for larger mass species with more complex structural features. Identities of trapped, misfolded intermediates and native-like peptide and protein structures can be more closely examined by means of chemically specific nucleation in the gas phase. As compared to previous works, multiple, distinct ion populations with differing HDX reactivity exist which strongly relate to clustering equilibrium. Future studies with larger biopolymers with this highly tunable workflow may offer a refined method to assess the conformational landscape associated with the flexibility of protein higher order structure.

Acknowledgements

The contributions by C. Hogan and T. Tamadate were supported by US NSF 2002852. H. Schramm and B. Clowers acknowledge the support provided by US NSF 2003042. We would also like to thank Dr. Stephen Valentine for helpful discussions regarding observations of multiple exchange rates within the drift tube ion mobility experiment.

Conflict of Interest

The authors declare no conflict of interest.

References

- (1) Hirsikko, A.; Nieminen, T.; Gagné, S.; Lehtipalo, K.; Manninen, H. E.; Ehn, M.; Hõrrak, U.; Kerminen, V.-M.; Laakso, L.; McMurry, P. H.; Mirme, A.; Mirme, S.; Petäjä, T.; Tammet, H.; Vakkari, V.; Vana, M.; Kulmala, M. Atmospheric Ions and Nucleation: A Review of Observations. *Atmos. Chem. Phys.* **2011**, *11* (2), 767–798.
- (2) Smith, J. N.; Barsanti, K. C.; Friedli, H. R.; Ehn, M.; Kulmala, M.; Collins, D. R.; Scheckman, J. H.; Williams, B. J.; McMurry, P. H. Observations of Aminium Salts in Atmospheric Nanoparticles and Possible Climatic Implications. *Proc. Natl. Acad. Sci. U. S. A.* **2010**, *107* (15), 6634–6639.
- (3) Pitteri, S. J.; McLuckey, S. A. Recent Developments in the Ion/ion Chemistry of High-Mass Multiply Charged Ions. *Mass Spectrom. Rev.* **2005**, *24* (6), 931–958.
- (4) Mehta, P.; Barboun, P.; Go, D. B.; Hicks, J. C.; Schneider, W. F. Catalysis Enabled by Plasma Activation of Strong Chemical Bonds: A Review. *ACS Energy Lett.* **2019**, *4* (5), 1115–1133.
- (5) Gary, S. P. Electromagnetic Ion/ion Instabilities and Their Consequences in Space Plasmas: A Review. *Space Sci. Rev.* **1991**, *56* (3), 373–415.
- (6) Herbst, E. Unusual Chemical Processes in Interstellar Chemistry: Past and Present. *Frontiers in Astronomy and Space Sciences* **2021**, 8. https://doi.org/10.3389/fspas.2021.776942.
- (7) Wakelam, V.; Bron, E.; Cazaux, S.; Dulieu, F.; Gry, C.; Guillard, P.; Habart, E.; Hornekær, L.; Morisset, S.; Nyman, G.; Pirronello, V.; Price, S. D.; Valdivia, V.; Vidali, G.; Watanabe, N. H2 Formation on Interstellar Dust Grains: The Viewpoints of Theory, Experiments, Models and Observations. *Molecular Astrophysics* **2017**, *9*, 1–36.
- (8) Parker, D. S. N.; Kaiser, R. I.; Troy, T. P.; Ahmed, M. Hydrogen Abstraction/acetylene Addition Revealed. *Angew. Chem. Int. Ed Engl.* **2014**, *53* (30), 7740–7744.
- (9) Kathmann, S. M.; Schenter, G. K.; Garrett, B. C. Ion-Induced Nucleation: The Importance of Chemistry. *Phys. Rev. Lett.* **2005**, *94* (11), 116104.
- (10) Kirkby, J.; Duplissy, J.; Sengupta, K.; Frege, C.; Gordon, H.; Williamson, C.; Heinritzi, M.; Simon, M.; Yan, C.; Almeida, J.; Tröstl, J.; Nieminen, T.; Ortega, I. K.; Wagner, R.; Adamov, A.; Amorim, A.; Bernhammer, A.-K.; Bianchi, F.; Breitenlechner, M.; Brilke, S.; Chen, X.; Craven, J.; Dias, A.; Ehrhart, S.; Flagan, R. C.; Franchin, A.; Fuchs, C.; Guida, R.; Hakala, J.; Hoyle, C. R.; Jokinen, T.; Junninen, H.; Kangasluoma, J.; Kim, J.; Krapf, M.; Kürten, A.; Laaksonen, A.; Lehtipalo, K.; Makhmutov, V.; Mathot, S.; Molteni, U.; Onnela, A.; Peräkylä, O.; Piel, F.; Petäjä, T.; Praplan, A. P.; Pringle, K.; Rap, A.; Richards, N. A. D.; Riipinen, I.; Rissanen, M. P.; Rondo, L.; Sarnela, N.; Schobesberger, S.; Scott, C. E.; Seinfeld, J. H.; Sipilä, M.; Steiner, G.; Stozhkov, Y.; Stratmann, F.; Tomé, A.; Virtanen, A.; Vogel, A. L.; Wagner, A. C.; Wagner, P. E.; Weingartner, E.; Wimmer, D.; Winkler, P. M.; Ye, P.; Zhang, X.; Hansel, A.; Dommen, J.; Donahue, N. M.; Worsnop, D. R.; Baltensperger, U.; Kulmala, M.; Carslaw, K. S.; Curtius, J. Ion-Induced Nucleation of Pure Biogenic Particles. *Nature* 2016, 533 (7604), 521–526.
- (11) Shuman, N. S.; Hunton, D. E.; Viggiano, A. A. Ambient and Modified Atmospheric Ion Chemistry: From Top to Bottom. *Chem. Rev.* **2015**, *115* (10), 4542–4570.
- (12) Zettergren, H.; Domaracka, A.; Schlathölter, T.; Bolognesi, P.; Díaz-Tendero, S.; Łabuda, M.; Tosic, S.; Maclot, S.; Johnsson, P.; Steber, A.; Tikhonov, D.; Castrovilli, M. C.; Avaldi, L.; Bari, S.; Milosavljević, A. R.; Palacios, A.; Faraji, S.; Piekarski, D. G.; Rousseau, P.; Ascenzi, D.; Romanzin, C.; Erdmann, E.; Alcamí, M.; Kopyra, J.; Limão-Vieira, P.; Kočišek, J.; Fedor, J.; Albertini, S.; Gatchell, M.; Cederquist, H.; Schmidt, H. T.; Gruber, E.; Andersen, L. H.; Heber, O.; Toker, Y.; Hansen, K.; Noble, J. A.; Jouvet, C.; Kjær, C.; Nielsen, S. B.; Carrascosa, E.; Bull, J.; Candian, A.; Petrignani, A. Roadmap on Dynamics

- of Molecules and Clusters in the Gas Phase. Eur. Phys. J. D 2021, 75 (5), 152.
- (13) Stein, T.; Jose, J. Molecular Formation upon Ionization of van Der Waals Clusters and Implication to Astrochemistry. *Isr. J. Chem.* **2020**, *60* (8-9), 842–849.
- (14) Metzger, S.; Lelieveld, J. Reformulating Atmospheric Aerosol Thermodynamics and Hygroscopic Growth into Fog, Haze and Clouds. *Atmos. Chem. Phys.* **2007**, *7* (12), 3163–3193.
- (15) Ishiyama, T.; Tahara, T.; Morita, A. Why the Photochemical Reaction of Phenol Becomes Ultrafast at the Air-Water Interface: The Effect of Surface Hydration. *J. Am. Chem. Soc.* **2022**, *144* (14), 6321–6325.
- (16) Riva, M.; Sun, J.; McNeill, V. F.; Ragon, C.; Perrier, S.; Rudich, Y.; Nizkorodov, S. A.; Chen, J.; Caupin, F.; Hoffmann, T.; George, C. High Pressure Inside Nanometer-Sized Particles Influences the Rate and Products of Chemical Reactions. *Environ. Sci. Technol.* **2021**, *55* (12), 7786–7793.
- (17) Adams, N. G.; Smith, D. The Selected Ion Flow Tube (SIFT); A Technique for Studying Ion-Neutral Reactions. *Int. J. Mass Spectrom. Ion Phys.* **1976**, *21* (3), 349–359.
- (18) Niedner-Schatteburg, G.; Bondybey, V. E. FT-ICR Studies of Solvation Effects in Ionic Water Cluster Reactions. *Chem. Rev.* **2000**, *100* (11), 4059–4086.
- (19) Maiβer, A.; Hogan, C. J., Jr. Examination of Organic Vapor Adsorption onto Alkali Metal and Halide Atomic Ions by Using Ion Mobility Mass Spectrometry. *Chemphyschem* **2017**, *18* (21), 3039–3046.
- (20) Oberreit, D.; Rawat, V. K.; Larriba-Andaluz, C.; Ouyang, H.; McMurry, P. H.; Hogan, C. J., Jr. Analysis of Heterogeneous Water Vapor Uptake by Metal Iodide Cluster Ions via Differential Mobility Analysis-Mass Spectrometry. *J. Chem. Phys.* **2015**, *143* (10), 104204.
- (21) Johnson, C. J.; Johnson, M. A. Vibrational Spectra and Fragmentation Pathways of Size-Selected, D2-Tagged Ammonium/methylammonium Bisulfate Clusters. *J. Phys. Chem. A* **2013**, *117* (50), 13265–13274.
- (22) Asmis, K. R.; Neumark, D. M. Vibrational Spectroscopy of Microhydrated Conjugate Base Anions. *Acc. Chem. Res.* **2012**, *45* (1), 43–52.
- (23) Wang, X.-B. Cluster Model Studies of Anion and Molecular Specificities via Electrospray Ionization Photoelectron Spectroscopy. *J. Phys. Chem. A* **2017**, *121* (7), 1389–1401.
- (24) Rawat, V. K.; Vidal-de-Miguel, G.; Hogan, C. J., Jr. Modeling Vapor Uptake Induced Mobility Shifts in Peptide Ions Observed with Transversal Modulation Ion Mobility Spectrometry-Mass Spectrometry. *Analyst* **2015**, *140* (20), 6945–6954.
- (25) Kwantwi-Barima, P.; Hogan, C. J., Jr; Clowers, B. H. Deducing Proton-Bound Heterodimer Association Energies from Shifts in Ion Mobility Arrival Time Distributions. *J. Phys. Chem. A* **2019**, *123* (13), 2957–2965.
- (26) Shi, L.; Holliday, A. E.; Glover, M. S.; Ewing, M. A.; Russell, D. H.; Clemmer, D. E. Ion Mobility-Mass Spectrometry Reveals the Energetics of Intermediates That Guide Polyproline Folding. *J. Am. Soc. Mass Spectrom.* **2016**, *27* (1), 22–30.
- (27) Westphall, M. S.; Lee, K. W.; Salome, A. Z.; Lodge, J. M.; Grant, T.; Coon, J. J. Three-Dimensional Structure Determination of Protein Complexes Using Matrix-Landing Mass Spectrometry. *Nat. Commun.* **2022**, *13* (1), 2276.
- (28) Engen, J. R.; Botzanowski, T.; Peterle, D.; Georgescauld, F.; Wales, T. E. Developments in Hydrogen/Deuterium Exchange Mass Spectrometry. *Anal. Chem.* **2021**, 93 (1), 567–582.
- (29) Houde, D.; Peng, Y.; Berkowitz, S. A.; Engen, J. R. Post-Translational Modifications Differentially Affect IgG1 Conformation and Receptor Binding. *Mol. Cell. Proteomics* **2010**, 9 (8), 1716–1728.
- (30) Shukla, A. K.; Westfield, G. H.; Xiao, K.; Reis, R. I.; Huang, L.-Y.; Tripathi-Shukla, P.; Qian, J.; Li, S.; Blanc, A.; Oleskie, A. N.; Dosey, A. M.; Su, M.; Liang, C.-R.; Gu, L.-L.; Shan, J.-M.; Chen, X.; Hanna, R.; Choi, M.; Yao, X. J.; Klink, B. U.; Kahsai, A. W.; Sidhu, S. S.; Koide, S.; Penczek, P. A.; Kossiakoff, A. A.; Woods, V. L., Jr; Kobilka, B. K.; Skiniotis, G.;

- Lefkowitz, R. J. Visualization of Arrestin Recruitment by a G-Protein-Coupled Receptor. *Nature* **2014**, *512* (7513), 218–222.
- (31) Dawicki-McKenna, J. M.; Langelier, M.-F.; DeNizio, J. E.; Riccio, A. A.; Cao, C. D.; Karch, K. R.; McCauley, M.; Steffen, J. D.; Black, B. E.; Pascal, J. M. PARP-1 Activation Requires Local Unfolding of an Autoinhibitory Domain. *Mol. Cell* **2015**, *60* (5), 755–768.
- (32) Khakinejad, M.; Kondalaji, S. G.; Maleki, H.; Arndt, J. R.; Donohoe, G. C.; Valentine, S. J. Combining Ion Mobility Spectrometry with Hydrogen-Deuterium Exchange and Top-down MS for Peptide Ion Structure Analysis. *J. Am. Soc. Mass Spectrom.* **2014**, *25* (12), 2103–2115.
- (33) Campbell, S.; Rodgers, M. T.; Marzluff, E. M.; Beauchamp, J. L. Deuterium Exchange Reactions as a Probe of Biomolecule Structure. Fundamental Studies of Gas Phase H/D Exchange Reactions of Protonated Glycine Oligomers with D2O, CD3OD, CD3CO2D, and ND3. *J. Am. Chem. Soc.* **1995**, *117* (51), 12840–12854.
- (34) Valentine, S. J.; Clemmer, D. E. H/D Exchange Levels of Shape-Resolved Cytochrome c Conformers in the Gas Phase. *J. Am. Chem. Soc.* **1997**, *119* (15), 3558–3566.
- (35) Valentine, S. J.; Clemmer, D. E. Temperature-Dependent H/D Exchange of Compact and Elongated Cytochrome c lons in the Gas Phase. *J. Am. Soc. Mass Spectrom.* **2002**, *13* (5), 506–517.
- (36) Kwantwi-Barima, P.; Ouyang, H.; Hogan, C. J., Jr; Clowers, B. H. Tuning Mobility Separation Factors of Chemical Warfare Agent Degradation Products via Selective Ion-Neutral Clustering. *Anal. Chem.* **2017**, *89* (22), 12416–12424.
- (37) Kwantwi-Barima, P.; Hogan, C. J., Jr; Clowers, B. H. Probing Gas-Phase-Clustering Thermodynamics with Ion Mobility-Mass Spectrometry: Association Energies of Phenylalanine Ions with Gas-Phase Alcohols. *J. Am. Soc. Mass Spectrom.* **2020**, *31* (9), 1803–1814.
- (38) Li, C.; Hogan; Jr.; J., C. Vapor Specific Extents of Uptake by Nanometer Scale Charged Particles. *Aerosol Sci. Technol.* **2017**, *51* (5), 653–664.
- (39) Hogan, C. J., Jr; Fernandez de la Mora, J. Ion-Pair Evaporation from Ionic Liquid Clusters. *J. Am. Soc. Mass Spectrom.* **2010**, *21* (8), 1382–1386.
- (40) Zapadinsky, E.; Passananti, M.; Myllys, N.; Kurtén, T.; Vehkamäki, H. Modeling on Fragmentation of Clusters inside a Mass Spectrometer. *J. Phys. Chem. A* **2019**, *123* (2), 611–624.
- (41) Mortensen, D. N.; Williams, E. R. Theta-Glass Capillaries in Electrospray Ionization: Rapid Mixing and Short Droplet Lifetimes. *Anal. Chem.* **2014**, *86* (18), 9315–9321.
- (42) Suckau, D.; Shi, Y.; Beu, S. C.; Senko, M. W.; Quinn, J. P.; Wampler, F. M., 3rd; McLafferty, F. W. Coexisting Stable Conformations of Gaseous Protein Ions. *Proc. Natl. Acad. Sci. U. S. A.* **1993**, *90* (3), 790–793.
- (43) Rand, K. D.; Pringle, S. D.; Murphy, J. P., 3rd; Fadgen, K. E.; Brown, J.; Engen, J. R. Gas-Phase Hydrogen/deuterium Exchange in a Traveling Wave Ion Guide for the Examination of Protein Conformations. *Anal. Chem.* **2009**, *81* (24), 10019–10028.
- (44) Rozman, M.; Kazazić, S.; Klasinc, L.; Srzić, D. Kinetics of Gas-Phase Hydrogen/deuterium Exchange and Gas-Phase Structure of Protonated Phenylalanine, Proline, Tyrosine and Tryptophan. *Rapid Commun. Mass Spectrom.* **2003**, *17* (24), 2769–2772.
- (45) Gard, E.; Willard, D.; Bregar, J.; Green, M. K.; Lebrilla, C. B. Site Specificity in the H-D Exchange Reactions of Gas-Phase Protonated Amino Acids with CH3OD. *J. Mass Spectrom.* **1993**, *28* (12), 1632–1639.
- (46) Reinecke, T.; Clowers, B. H. Implementation of a Flexible, Open-Source Platform for Ion Mobility Spectrometry. *HardwareX* **2018**, *4*, e00030.
- (47) Kwantwi-Barima, P.; Reinecke, T.; Clowers, B. H. Increased Ion Throughput Using Tristate Ion-Gate Multiplexing. *Analyst* **2019**, *144* (22), 6660–6670.
- (48) Morrison, K. A.; Siems, W. F.; Clowers, B. H. Augmenting Ion Trap Mass Spectrometers

- Using a Frequency Modulated Drift Tube Ion Mobility Spectrometer. *Anal. Chem.* **2016**, *88* (6), 3121–3129.
- (49) Kwantwi-Barima, P.; Hogan, C. J., Jr; Clowers, B. H. Deducing Proton-Bound Heterodimer Association Energies from Shifts in Ion Mobility Arrival Time Distributions. *J. Phys. Chem. A* **2019**, *123* (13), 2957–2965.
- (50) Wagner, D. S.; Melton, L. G.; Yan, Y.; Erickson, B. W.; Anderegg, R. J. Deuterium Exchange of Alpha-Helices and Beta-Sheets as Monitored by Electrospray Ionization Mass Spectrometry. *Protein Sci.* **1994**, *3* (8), 1305–1314.
- (51) Sawyer, H. A.; Marini, J. T.; Stone, E. G.; Ruotolo, B. T.; Gillig, K. J.; Russell, D. H. The Structure of Gas-Phase Bradykinin Fragment 1–5 (RPPGF) lons: An Ion Mobility Spectrometry and H/D Exchange Ion-Molecule Reaction Chemistry Study. *J. Am. Soc. Mass Spectrom.* **2005**, *16* (6), 893–905.
- (52) Jekel, C. F.; Venter, G. PWLF: A Python Library for Fitting 1D Continuous Piecewise Linear Functions. **2019**.
- (53) Gard, E.; Green, M. K.; Bregar, J.; Lebrilla, C. B. Gas-Phase Hydrogen/deuterium Exchange as a Molecular Probe for the Interaction of Methanol and Protonated Peptides. *J. Am. Soc. Mass Spectrom.* **1994**, *5* (7), 623–631.
- (54) Ranasinghe, A.; Cooks, R. G.; Sethi, S. K. Selective Isotopic Exchange of Polyfunctional Ions in Tandem Mass Spectrometry: Methodology, Applications and Mechanism. *J. Mass Spectrom.* **1992**, *27* (2), 77–88.
- (55) M. K. Green and C. B. Lebrilla. The Role of Proton-Bridged Intermediates in Promoting Hydrogen-Deuterium Exchange in Gas-Phase Protonated Diamines, Peptides and Proteins. *Int. J. Mass Spectrom. Ion Process.* **1998**, *175* (1-2), 15–26.
- (56) Dias, H. J.; Bento, M. V. B.; da Silva, É. H.; Saturnino-Júnior, A.; de Oliveira, M. F.; Vessecchi, R.; Parreira, R. L. T.; Crotti, A. E. M. Gas-Phase Fragmentation Reactions of Protonated Cocaine: New Details to an Old Story. *J. Mass Spectrom.* **2018**, *53* (3), 203–213.
- (57) Polfer, N. C.; Dunbar, R. C.; Oomens, J. Observation of Zwitterion Formation in the Gas-Phase H/D-Exchange with CH(3)OD: Solution-Phase Structures in the Gas Phase. *J. Am. Soc. Mass Spectrom.* **2007**, *18* (3), 512–516.
- (58) Westheimer, F. H. The Magnitude of the Primary Kinetic Isotope Effect for Compounds of Hydrogen and Deuterium. *Chem. Rev.* **1961**, *61* (3), 265–273.